doi: 10.37905/jgeosrev.v8i1.35609 ejurnal.ung.ac.id/index.php/jgeosrev

Vol. 8, No. 1, January 2026: 129-138

Jambura Geoscience Review

p-ISSN 2623-0682 | e-ISSN 2656-0380

Department of Earth Science and Technology, Universitas Negeri Gorontalo

Identification of Landslide-Prone Areas and Slip Zones Along the National Road in Bunut, Kapuas District, Sanggau Regency

Ikdham Nurul Khalik[1], Rossie W. Nusantara[2], Nurhayati[3]

[1] *Environmental Science Master Program, Universitas Tanjungpura, Jl. Prof. Dr. H Jl. Profesor Dokter H. Hadari Nawawi, Pontianak, West Kalimantan, 78124, Indonesia*

[2] *Soil Science Study Program, Universitas Tanjungpura, Jl. Prof. Dr. H Jl. Profesor Dokter H. Hadari Nawawi, Pontianak, West Kalimantan, 78124, Indonesia*

[3] *Civil Engineering Master Program, Universitas Tanjungpura, Jl. Prof. Dr. H Jl. Profesor Dokter H. Hadari Nawawi, Pontianak, West Kalimantan, 78124, Indonesia*

ARTICLE INFO

Article history:
Received: 25 November 2025
Accepted: 6 January 2026
Published: 15 January 2026

Keywords:
Geoelectrical resistivity; Landslide; Slip surface; Slope stability; Wenner–Schlumberger

Corresponding author:
Ikdham Nurul Khalik
Email: ikdham.n.khalik@gmail.com

Read online:
Scan this QR code with your smart phone or mobile device to read online.

ABSTRACT

Landslides repeatedly disrupt the national road corridor in Bunut Sub-District, Kapuas District, Sanggau Regency (West Kalimantan), indicating that slope failure is strongly controlled by subsurface conditions that cannot be reliably inferred from surface observations alone. This study delineates landslide-prone segments and interprets the subsurface slip surface using 2D electrical resistivity imaging with the Wenner–Schlumberger array. Field measurements were conducted along three 120 m survey lines using 13 electrodes with 10 m spacing, and the data were inverted (Res2Dinv) to obtain true-resistivity sections for each line. Interpretation was guided by published resistivity classifications and the local geomorphological setting. The resistivity models reveal a clear stratification of near-surface materials, with low-resistivity zones (<300 Ωm) interpreted as water-saturated, clay-rich layers and higher-resistivity zones representing comparatively drier and more permeable materials. The slip surface is consistently expressed as a sharp resistivity contrast and is interpreted at resistivity values of approximately 300–2400 Ωm at depths of about 6–18 m below ground level, suggesting a mechanically weak interface that is prone to shear under intense rainfall and pore-pressure increase. These results provide spatial constraints on slip-zone geometry that can be used to support hazard zoning and to prioritize mitigation along the road section, particularly through improved drainage, surface-water control, and slope management at locations where saturated low-resistivity materials underlie permeable surficial deposits.

How to cite: Khalik, IN. (2026). Identification of Landslide-Prone Areas and Slip Zones Along the National Road in Bunut, Kapuas District, Sanggau Regency. *Jambura Geoscience Review, 8*(1), 129-138. https://doi.org/10.37905/jgeosrev.v8i1.35609

1. INTRODUCTION

Landslides are among the most frequent natural disasters in Indonesia, particularly in hilly and mountainous regions during the rainy season. Recent studies indicate that areas characterized by steep slopes and high annual rainfall are highly susceptible to landslide occurrence (Naryanto et al., 2020; Satyaningsih et al., 2023). Landslide events are controlled by a combination of natural factors, including lithology, soil properties, slope gradient, land cover, groundwater conditions, and rainfall intensity, as well as anthropogenic activities such as unregulated land-use change, deforestation, and infrastructure development on steep terrain (Hsu, 2020; Putra et al., 2025). These

conditions often lead to severe impacts, including casualties, property loss, and damage to critical infrastructure such as roads, bridges, and settlements.

Slope instability is strongly influenced by subsurface geological and hydrological conditions. Among the controlling factors, the presence of a slip plane plays a critical role in triggering landslides. The slip plane generally forms at the boundary between weathered soil layers and underlying impermeable bedrock, where water accumulation increases pore water pressure and reduces shear strength. Recent geotechnical studies emphasize that identifying the depth and geometry of slip planes is essential for slope stability assessment and effective landslide mitigation planning (Hsu, 2020; Sholichin et al., 2024). In recent Indonesian case studies, landslide assessment has increasingly combined surface-based susceptibility evaluation with engineering-geology evidence to improve interpretability and decision relevance for mitigation (Santoso et al., 2020; Juwono et al., 2022; Pambudi et al., 2022).

The research area, located in Bunut Sub-District, Kapuas District, Sanggau Regency, experiences an average annual rainfall of approximately 3,080 mm, which places the region in a high landslide susceptibility category. Official disaster documentation also indicates repeated landslide occurrences in Sanggau Regency during recent years (BNPB, 2021). One significant landslide occurred on 10 February 2022 along the national road, causing damage to approximately 50 meters of roadway and displacing a nearby power pole. This event was mainly triggered by intense rainfall and unfavorable local geological conditions, suggesting the presence of a subsurface slip zone controlling slope failure.

From a hazard-management perspective, the core scientific and practical problem is that road-slope failures are often managed using surface indicators (scarps, cracks, drainage issues) without sufficiently constraining the controlling subsurface architecture—especially the depth, continuity, and material contrast associated with the slip plane. A general solution therefore requires an investigation framework that links (i) rainfall-driven triggering processes and stability degradation (Hsu, 2020), with (ii) subsurface evidence capable of delineating the likely failure interface and related hydrogeological controls, thereby enabling defensible zoning and targeted mitigation actions.

Subsurface characterization is therefore crucial for understanding landslide mechanisms in the study area. Geoelectrical resistivity methods have been widely applied in recent landslide and geotechnical studies due to their ability to identify lithological contrasts, groundwater saturation zones, and impermeable layers associated with slip plane development (Sedana et al., 2015; Zulfahmi et al., 2025). Variations in electrical resistivity reflect differences in material composition, moisture content, and degree of compaction, making the method effective for detecting subsurface conditions related to slope instability.

Geoelectrical imaging is particularly useful in tropical settings where weathering profiles, perched water, and clay-rich horizons can create strong resistivity contrasts relevant to slip-surface development. Prior applications in Indonesia demonstrate that resistivity-based interpretation can support engineering and hazard investigations by distinguishing relatively permeable layers from saturated or clay-dominated zones that may act as potential detachment horizons (As'ari et al., 2020; Daniswara et al., 2020).

In addition, recent applied studies emphasize that the interpretive value of resistivity sections increases when the subsurface model is explicitly connected to slope-forming processes and site constraints, thereby improving the relevance of outputs for risk reduction and design decisions (Juwono et al., 2022; Pambudi et al., 2022). Within this perspective, resistivity imaging serves not merely as mapping, but as a mechanism-oriented tool to infer where water accumulation and material contrasts likely concentrate shear deformation.

While prior studies provide methodological foundations, their location-specific variability in lithology, geomorphology, and triggering regimes limits direct application to the Bunut national-road corridor (Daniswara et al., 2020; Santoso et al., 2020). Local validation is needed to translate resistivity imaging into constraints on slip-plane geometry (Sedana et al., 2015; Juwono et al., 2022; Yuniawan et al., 2022). Despite frequent landslides along the Bunut national road, subsurface slip plane geometry and depth remain unidentified, highlighting the need for geophysical investigation to support mitigation efforts.

This study aims to identify slip plane zones using geoelectrical resistivity in the landslide-prone area along the national road in Bunut, Kapuas District, Sanggau Regency, West Kalimantan. The geoelectrical method will provide subsurface information on resistivity distribution, slip plane depth, and lithological boundaries that address the research objective. The novelty lies in providing site-specific constraints on the depth and geometry of the inferred slip zone under a high-rainfall tropical setting, strengthening the basis for landslide-prone zoning along the affected national road segment (BNPB, 2021; Naryanto et al., 2020).

2. METHOD

2.1. Study Area and Period

Administratively, the study area is located along the national road corridor in Bunut Sub-District, Kapuas District, Sanggau Regency, West Kalimantan, Indonesia. Field activities were conducted from July to September 2022 and focused on a road-slope segment that has experienced repeated landslides. Site reconnaissance was performed to document accessibility and surface conditions, and to determine the most representative positions for geoelectrical survey lines along the affected corridor.

Figure 1. Road access to the study area

2.2. Tools and Materials

The instruments used in this study included an electrical resistivity imaging system (IRES T300F), a 12 V power supply, electrodes and multicore cables, and supporting tools for electrode installation and distance control. Field positioning and documentation were supported by a handheld GPS and field notes. Data processing and mapping were conducted using Res2Dinv for 2D inversion, Slide 5.0 for slope-related interpretation, and QGIS for spatial visualization and map preparation (As'ari et al., 2020).

2.3. Slip Plane and Soil Profile Data Acquisition

Slip-plane and soil-profile information was acquired using 2D geoelectrical resistivity surveying to characterize subsurface contrasts that may indicate weak zones and potential detachment interfaces (Pambudi et al., 2022). Measurements were conducted along three survey lines (Line 1–Line 3). Each line was 120 m long using 13 electrodes with 10 m spacing, and data were collected to obtain apparent resistivity values at increasing investigation depths.

The Wenner–Schlumberger array was applied because it provides sensitivity to both lateral and vertical resistivity variations and is commonly used for near-surface engineering and landslide investigations (Daniswara et al., 2020). Survey-line placement considered slope morphology, surface drainage, and evidence of previous landslide activity to ensure that the measurements captured subsurface conditions relevant to slope instability (Juwono et al., 2022).

Data quality control during acquisition included checking electrode contact conditions and signal stability, repeating measurements when needed, and excluding noisy or unstable readings prior to inversion to maintain data reliability.

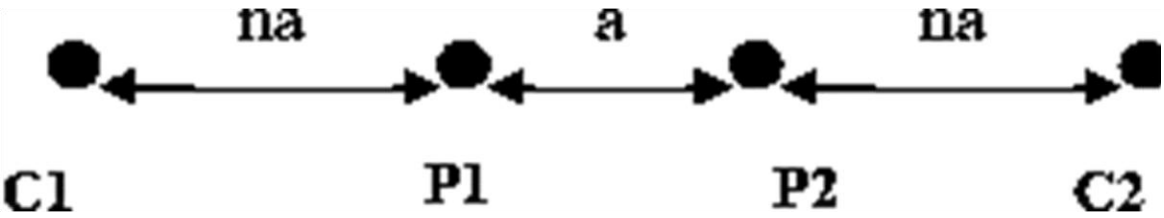

Figure 2. Electrode configuration scheme used in the Wenner–Schlumberger configuration

2.4. Data Processing

Apparent resistivity data were processed using Res2Dinv. The inversion procedure iteratively updates a subsurface resistivity model to obtain a 2D true-resistivity section that best fits the observed data. The resulting resistivity sections were then used as the primary basis for interpreting subsurface layering and potential slip-plane geometry.

2.5. Data Analysis and Interpretation Parameters

Interpretation of subsurface materials was carried out by relating the inverted resistivity ranges to lithological and hydrogeological characteristics using established resistivity classification references (Table 1 and Table 2). Low resistivity values were interpreted to represent clay-rich and/or water-saturated materials, while higher resistivity values were interpreted to reflect relatively drier and more competent units (Santoso et al., 2020).

Because no direct subsurface validation was available, interpretation was strengthened through consistency checks against surface observations and geomorphological context. Statistical analysis was not applied because the study relied on deterministic 2D inversion outputs and geological interpretation rather than inferential statistical testing.

Table 1. Rock resistivity classification

Rock / Soil Type	Resistivity Range (Ω.m)
Wet soft clay	1,5 - 3,0
Silt soil and wet soft silt	3 - 15
Sandy silt soil	15 - 150
Jointed bedrock containing moist soil	150 -300
Sand and gravel with silt layers	± 300
Bedrock containing dry soil	300 -2400
Unweathered bedrock	>2400

Table 2. Soil resistivity classification

Rock / Soil Type	Resistivity Range (Ω m)
Clay	1- 100
Silt	10- 200
Marls	3- 70
Quartz	500-8.00.000
Sandstone	200-8.000
Limestone	500- 10.000
Shales	20-2.000
Groundwater	0,5- 300
Seawater	0,2
Gravel	100-600
Andesite	$1{,}7\times10^{2}$ - 45×10^{4}
Alluvial deposits	10-800
Granite	200-10.000

Source: Santoso et al., 2020

3. RESULTS AND DISCUSSION

3.1. Results

Figure 3. Geoelectrical survey line based on satellite imagery

The field measurement data in the form of rock resistivity values were processed using Res2Dinv software, resulting in a two-dimensional vertical subsurface profile for each survey line. The resistivity values in these profiles represent the types of subsurface materials present in the study area. The geoelectrical measurement results obtained at the landslide site show resistivity values ranging from 0.14 to 2849 Ωm on line 1, 24.4 to 630 Ωm on line 2, and 25.7 to 447 Ωm on line 3 (Figure 3).

In the next stage, the resistivity values from each survey line were correlated with rock resistivity classification and geological conditions of the study area to visualize the subsurface soil and rock profiles. The two-dimensional geoelectrical profiles of the soil and rock for each line, obtained by correlating resistivity data with rock resistivity classes and regional geology, are presented in Figure 4.

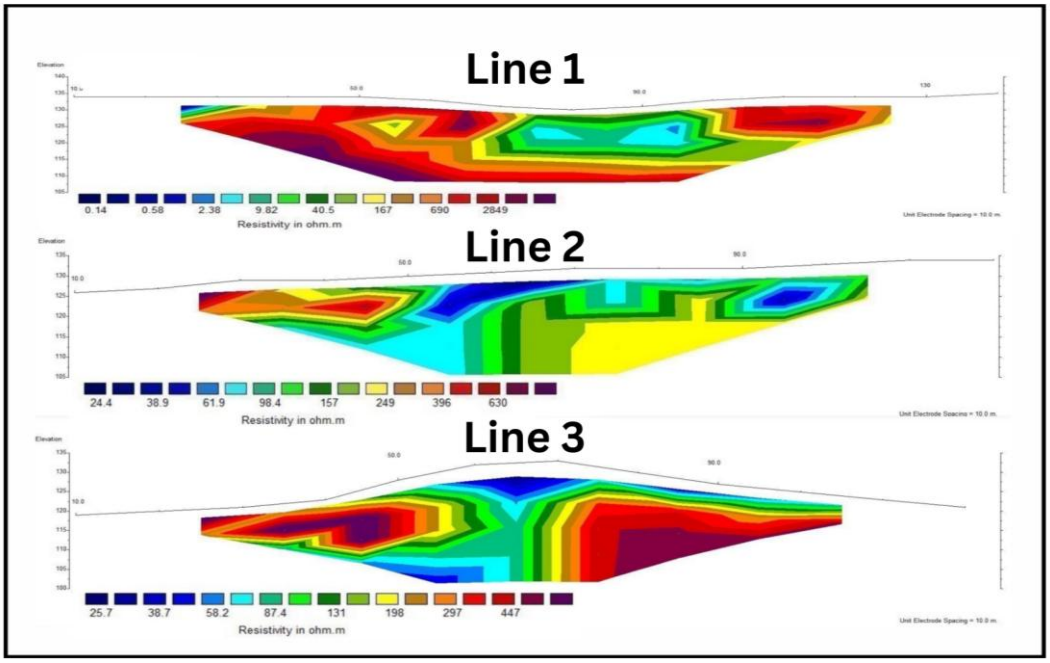

Figure 4. 2D geoelectrical profile showing soil structure and slip plane interpretation

To support consistent lithological interpretation across all lines, the resistivity ranges were grouped into operational classes used in this study (Table 3). These classes were then used to interpret contrasts observed in the 2D sections and to delineate the inferred slip-surface zone.

Table 3. Classification of resistivity values

Color	Resistivity Range (Ωm)	Rock / Soil Type
	< 15	Silty soil - Wet clay
	15 - 100	Soft, wet silty clay
	100 - 150	Sandy siltstone
	150 - 300	Fractured sandstone containing water
	300 - 2400	Dry sandstone (massive and impermeable)

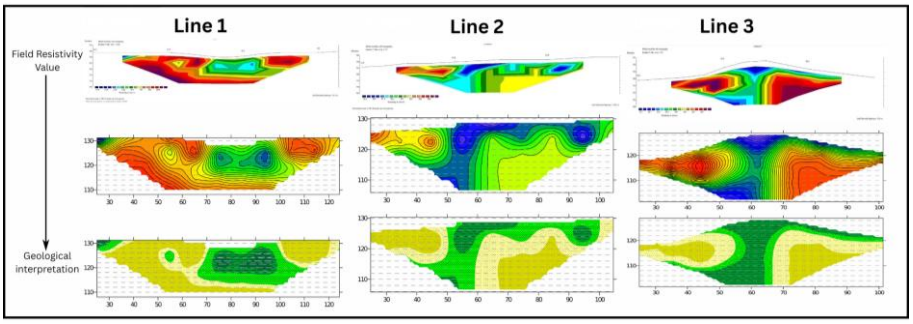

Figure 5. Geological interpretation and processed 2D geoelectrical cross-section

The geoelectrical survey was employed to obtain a more detailed characterization of the subsurface conditions and to estimate both the depth and geometry of the landslide slip plane through the analysis of resistivity variations between subsurface layers. The results reveal a pronounced resistivity contrast within the landslide zone, indicating a clear boundary between the overlying displaced material and the underlying stable layer. The material above the interpreted slip surface is characterized by moderate resistivity values, which are commonly associated with relatively dry, fractured, or loosely consolidated soil and rock masses. In contrast, the layer beneath the slip surface exhibits significantly lower resistivity, suggesting the presence of water-saturated materials, clay-rich deposits, or highly weathered zones that reduce shear strength. The slip plane itself is interpreted as a concave-shaped boundary, reflecting the typical geometry of rotational landslides, where movement occurs along a curved failure surface. This concave geometry implies progressive downslope displacement controlled by subsurface lithology and hydrological conditions. Overall, the identified resistivity contrast and slip plane geometry provide strong geophysical evidence for the mechanism of slope instability and contribute to a more reliable assessment of landslide behavior and potential reactivation zones.

In this study, the slip plane is interpreted as a boundary within sandstone layers exhibiting resistivity values ranging from 300 to 2400 Ωm. Beneath this boundary, a low-resistivity zone (<300 Ωm) is interpreted as a water-saturated and relatively impermeable layer composed of clay, silt, sandy siltstone, and fractured sandstone. This low-permeability layer likely facilitates groundwater accumulation, which contributes to reduced shear strength and promotes slope instability.

The topography along the survey line follows the natural slope inclination, and the depth of the interpreted slip plane is estimated to range from approximately 6 to 18 m below the ground surface. The geoelectrical profile from Line 1 indicates that the landslide material above the slip plane has an average thickness of about 6 m. Although no borehole data are available, the interpretation is supported by field observations, slope morphology, and lithological characteristics consistent with previous geoelectrical studies in landslide-prone areas.

The slip-plane delineation is further summarized through the cross-sectional and 3D visualization outputs shown in Figure 6.

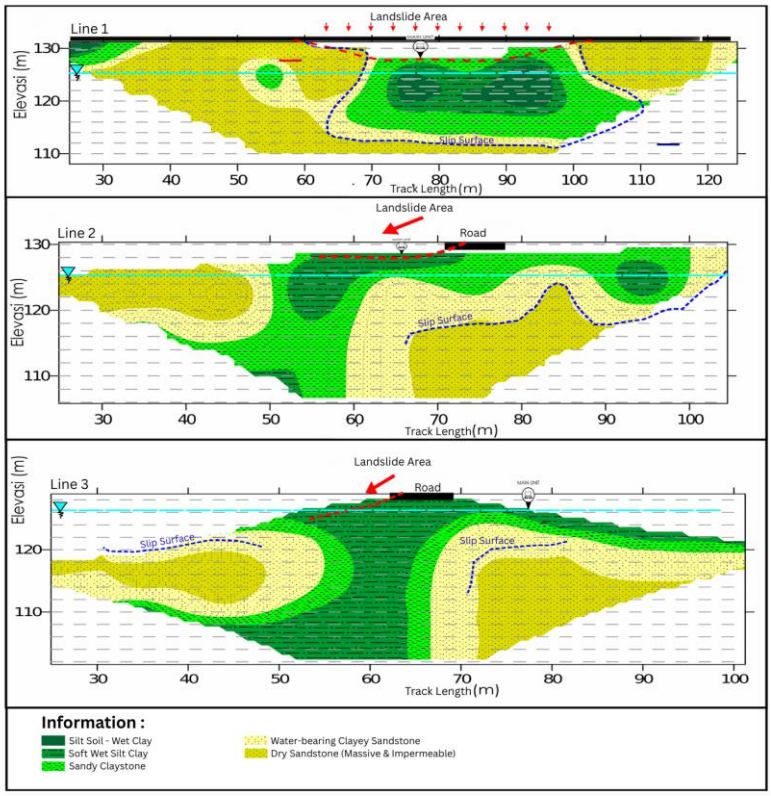

Figure 6. Results of slip plane analysis on the 2D cross-section

3.2. Discussion

The general geological condition of the area where geoelectrical measurements were conducted is dominated by the Sekayam Sandstone Formation (Tos) of Oligocene age. This formation is characterized by massive and compact sandstone interbedded with mudstone, claystone, and shale layers. The sandstone is typically medium to coarse-grained lithic arenite, grayish-green in color, and locally conglomeratic. The main constituents include quartz, lithic fragments (basalt, quartzite, and metamorphic rock fragments), with minor feldspar, mica, and dark minerals. The rock exhibits planar cross-bedding, moderate sorting, and is carbonate-cemented. Intercalations of gray, red, or green mudstone layers occur with thicknesses less than 50 cm, and occasionally thin coal seams are present.

The geological condition of the study area is characterized by interbedded sandstone and claystone layers belonging to the Sekayam Sandstone Formation, with a moderate to high degree of weathering. Structurally, minor jointed rock layers were found throughout the investigation site. The distribution of the geoelectrical survey lines was designed to represent the entire study area to obtain comprehensive and accurate information about the regional geological subsurface conditions.

Within this geological framework, the resistivity pattern indicates a mechanically weak interface expressed as a sharp contrast between the inferred sandstone unit (moderately resistive) and the underlying saturated, low-resistivity materials (<300 Ωm). This configuration is consistent with rainfall-driven pore-pressure increase, where infiltration concentrates above a semi-impermeable boundary and promotes shear localization along the detachment surface (Hsu, 2020; Daniswara et al., 2020; Pambudi et al., 2022). The identified slip-plane depth (≈6–18 m) and the ~6 m average thickness of the mobilized material on Line 1 indicate that failure is not merely a shallow soil slide, but is controlled by subsurface layering and permeability contrasts that can sustain perched water conditions during prolonged rainfall.

The characteristics of the slip plane identified from the geoelectrical measurements are indicated by a pronounced contrast in resistivity between subsurface layers forming the slope. This resistivity break is interpreted as a lithological–hydrogeological boundary that commonly marks

mechanically weak interfaces and potential detachment zones in landslide-prone slopes (Akbar et al., 2021; Wiyuda et al., 2022). A clear resistivity contrast is observed between the sandstone layer and the overlying sandy clay to sandy silt materials. In hydrogeological terms, this contrast reflects differences in pore structure and water content, which can be used to infer relative permeability and groundwater behavior within the slope materials (Sugianti et al., 2022; Wumu et al., 2022). The massive sandstone layer is characterized by relatively low porosity and permeability, functioning as a semi-impermeable base, whereas the jointed sandstone and overburden soils exhibit higher porosity and permeability, enabling greater water infiltration and storage. Such a permeability contrast favors water accumulation above the semi-impermeable boundary and the development of elevated pore-water pressure along the interface, thereby promoting shear localization and slip-plane activation during rainfall (Mutaqin et al., 2023; Akbar et al., 2021).

During rainfall events, infiltrating water percolates through the soil cover and fractured sandstone, leading to water accumulation above the less permeable sandstone layer. This process increases the pore water pressure within the overlying materials and adds to the self-weight of the slope, thereby reducing effective stress and shear strength along the slip plane. As a result, slope stability decreases, and when the resisting forces are exceeded, slope failure in the form of a landslide may occur.

From a mitigation standpoint, the results emphasize that interventions should prioritize (i) limiting infiltration into the jointed/porous near-surface materials, and (ii) preventing water build-up above the lower-permeability layer that underlies the inferred slip plane. Practically, this supports mitigation options such as improved surface-water control and drainage management along the road cut and adjacent slope, combined with targeted stabilization at segments where low-resistivity saturated materials are laterally continuous beneath the road corridor (Sedana et al., 2015; Juwono et al., 2022).

4. CONCLUSIONS

The geoelectrical measurement results reveal five resistivity-based subsurface units along the landslide-prone national road segment in Bunut, ranging from silty soil–wet clay (<15 Ωm) to dry, massive sandstone (>300 Ωm). The layer interpreted as the slip surface consists of sandstone with resistivity values ranging from 300 to 2400 Ωm, while the underlying impermeable or water-saturated zone is inferred to comprise clay, silt, sandy siltstone, and jointed sandstone with resistivity values of <300 Ωm at depths of approximately 6–18 meters. The inferred geometry indicates that slope failure is primarily controlled by a permeability contrast that promotes groundwater accumulation and pore-pressure increase during intense rainfall. These results provide practical implications for slope stabilization, as the precise delineation of the slip surface and its controlling hydrogeological conditions can support targeted design of drainage systems and reinforcement structures to reduce pore-water pressures. Accordingly, landslide-prone zoning and mitigation along the corridor should prioritize surface- and subsurface-drainage improvement and localized stabilization where the saturated low-resistivity layer is laterally continuous beneath the road cut.

5. REFERENCES

Akbar, L., Lihawa, F., & Mahmud, M. (2021). Analisis Tipe Dan Bidang Gelincir Longsor Di Kabupaten Gorontalo Utara. *Jambura Geoscience Review*, *3*(2), 73-83. https://doi.org/10.34312/jgeosrev.v3i2.10623

As'ari, A., Tongkukut, S. H. J., Pogaga, B. A., Akasi, I. A., Sagai, F. S., & Loupatty, T. B. (2019). Investigasi Akuifer Air Tanah di Banua Buha Asri 1 Kelurahan Buha Manado Dengan Menggunakan Metode Geolistrik Resistivitas. *Jurnal Ilmiah Sains, 20*(1), 1–5. https://doi.org/10.35799/jis.20.1.2020.25143

BNPB. (2021). BNPB (Badan Nasional Penanggulangan Bencana). Data & Informasi Bencana Indonesia (Online). https://bnpb.go.id/ diakses : 20 Maret 2021

Daniswara, A., Dahrin, D., & Setianingsih, S. (2020). Analysis And Modelling Of Geoelectric Data Modeling For The Identication Of Groundwater aquifer At Cisarua Area, West Bandung. *Jurnal Geofisika, 17*(2), 22-25. https://10.36435/jgf.v17i2.416

Hsu, C.-F. (2023). Rainfall-Induced Landslide Susceptibility Assessment and the Establishment of Early Warning Techniques at Regional Scale. *Sustainability*, *15*(24), 16764. https://doi.org/10.3390/su152416764

Juwono, A. M., Susilo, A., Sunaryo, Aprilia, F., & Hisyam, F. (2022). Study of Subsurface Conditions of Southern Cross Road Using the Wenner-Schlumberger Method for Disaster Mitigation. International Journal of GEOMATE, 23(97), 97–105. https://doi.org/10.21660/2022.97.3261

Mutaqin, D., Hendarmawan, H., Haryanto, A., Mardiana, U., & Mohammad, F. (2023). Contribution of Resistivity Properties in Estimating Hydraulic Conductivity in Ciremai Volcanic Deposits. *Jambura Geoscience Review,* *5*(1), 51-62. doi:https://doi.org/10.34312/jgeosrev.v5i1.17333

Naryanto, H. S., Soewandita, H., Ganesha, D., Prawiradisastra, F., & Kristijono, A. (2019). Analisis Penyebab Kejadian dan Evaluasi Bencana Tanah Longsor di Desa Banaran, Kecamatan Pulung, Kabupaten Ponorogo, Provinsi Jawa Timur Tanggal 1 April 2017. *Jurnal Ilmu Lingkungan, 17*(2), 272-282. https://doi.org/10.14710/jil.17.2.272-282

Pambudi, R. R. ., Nurul, M. ., Prihadita, W. P. ., & Mulyasari, R. (2022). Comparison of The Electrode Configuration of The Resistivity Geoelectric Method for Landslide Analysis on Highway Suban, Bandar Lampung: Analisis Kelongsoran dengan Metode Geolistrik Konfigurasi Wenner-Schlumberger dan Wenner-Alpha di Jalan Raya Suban Bandar Lampung. *Jurnal Geocelebes*, *6*(2), 108 – 116. https://doi.org/10.20956/geocelebes.v6i2.17903

Putra, A. N., Jaenudin, Prasetya, N. R., Sugiarto, M. T., Sudarto, Prayogo, C., Maritimo, F., & Admajaya, F. T. (2025). Utilizing Remote Sensing and Random Forests to Identify Optimal Land Use Scenarios and Address the Increase in Landslide Susceptibility. *Sustainability*, *17*(9), 4227. https://doi.org/10.3390/su17094227

Santoso, B., Subagio, S., Hasanah, M. U., & Suwarga, H. (2020). Investigation Estimating of Land Movement Using Methods of Electrical Resistivity Tomography and Self-Potential in Pasanggrahan Baru Area, South Sumedang. *Jurnal Geologi Dan Sumberdaya Mineral, 21*(1), 33–44. https://doi.org/10.33332/jgsm.geologi.v21i1.497

Satyaningsih, R., Jetten, V., Ettema, J., Sopaheluwakan, A., Lombardo, L., & Nuryanto, D. E. (2023). Dynamic rainfall thresholds for landslide early warning in Progo Catchment, Java, Indonesia. *Natural Hazards, 119*, 2133–2158. https://doi.org/10.1007/s11069-023-06208-2

Sedana, D., As'ari, A., & Tanauma, A. (2015). Pemetaan Akuifer Air Tanah Di Jalan Ringroad Kelurahan Malendeng Dengan Menggunakan Metode Geolistrik Tahanan Jenis. *Jurnal Ilmiah Sains*, *15*(1), 33–37. https://doi.org/10.35799/jis.15.1.2015.6778

Sholichin, M., Othman, F., Prayogo, T. B., & Rahardjo, S. S. P. (2024). Assessing landslide susceptibility and formulating adaptation strategies in the Konto Watershed, East Java, Indonesia. *International Journal of Disaster Risk Reduction, 113*, 104797. https://doi.org/10.1016/j.ijdrr.2024.104797

Sugianti, K., Zainuri, A., & Hutagalung, R. (2022). Estimasi Potensi Cadangan Air Tanah Dengan Metode Persamaan Darcy di Desa Pilomonu, Gorontalo. *Journal of Applied Geoscience and Engineering, 1*(1), 23-36. doi:https://doi.org/10.34312/jage.v1i1.15505

Wiyuda, M., Samodra, S., & Utami, P. (2022). Investigasi Bawah Permukaan Pada Area Kawah Sikidang, Dieng, Jawa Tengah Menggunakan Metode Geolistrik. *Journal of Applied Geoscience and Engineering, 1*(2), 82-92. https://doi.org/10.34312/jage.v1i2.17343

Wumu, R., Zainuri, A., & Akase, N. (2022). Karakteristik Akuifer Menggunakan Metode Geolistrik Resistivity Di Kecamatan Kota Tengah Kota Gorontalo. *Jambura Geoscience Review, 4*(1), 60-68. doi:https://doi.org/10.34312/jgeosrev.v4i1.12752

Yuniawan, R. A., Rifa'i, A., Faris, F., Subiyantoro, A., Satyaningsih, R., Hidayah, A. N., Hidayat, R., Mushthofa, A., Ridwan, B. W., Priangga, E., Muntohar, A. S., Jetten, V. G., Westen, C. J. v., Bout, B. V. d., & Sutanto, S. J. (2022). Revised Rainfall Threshold in the Indonesian Landslide Early Warning System. *Geosciences*, *12*(3), 129. https://doi.org/10.3390/geosciences12030129

Zulfahmi, Z., Putra, M. H. Z., Sarah, D., Tohari, A., Madiutomo, N., Hartanto, P., & Damayanti, R. (2025). GIS-Based Landslide Susceptibility Mapping with a Blended Ensemble Model and Key Influencing Factors in Sentani, Papua, Indonesia. *Geosciences*, *15*(10), 390. https://doi.org/10.3390/geosciences15100390